Microchimica Acta
https://doi.org/10.1007/s00604-018-3204-9

ORIGINAL PAPER

Graphene oxide with in-situ grown Prussian Blue as an electrochemical probe for microRNA-122

Feng Wang[1,2] · Yaru Chu[2] · Yijing Ai[2] · Lin Chen[3] · Feng Gao[2]

Received: 10 October 2018 / Accepted: 23 December 2018

Abstract

An electrochemical biosensor for microRNA was constructed on the basis of direct growth of electroactive Prussian Blue (PB) on graphene oxide (GO). A mercapto-modified probe DNA that is complementary to the hepatocellular carcinoma biomarker microRNA-122 was firstly anchored on a gold electrode (AuE). Then, GO (with its large surface and multiple active sites) was adsorbed on probe DNA through π-interaction. Subsequently, the PB nanoparticles were directly grown on GO via alternative dipping the electrode in solutions of $FeCl_3$ and hexacyanoferrate(III). Upon incubation of the resulting electrode with a solution of microRNA-122, the probe DNA on the electrode interacts with microRNA-122 to form a rigid duplex. This results in the release of electroactive PB/GO from the sensing interface and a decrease in current, typically measured at 0.18 V (vs. Ag/AgCl (3 M KCl)). The sensor covers the 10 fM to 10 nM microRNA-122 concentration range and has a 1.5 fM detection limit. The method was successfully applied to the determination of microRNA-122 in real biological samples.

Keywords UV-vis spectra · Scanning electron microscopy · Atomic force microscopy · π-stacking · Base-pairing principle · Nanosize effect · Liver injury biomarker

Introduction

MicroRNA-122 is an abundant and highly liver-specific microRNA [1]. The levels of microRNA-122 are positively correlated with liver transaminases and negatively correlated with the Model for End-Stage Liver Disease (MELD) score [2]. Hence, microRNA-122 is a biomarker for liver injury. So, the rapid, sensitive and accurate analysis of microRNA-122 is very significant in early warning and prognosis of liver-related diseases On the basis of base-pairing principle of A-U and G-C bases, the hybridization-dependent electrochemical strategy attracts wide interest in microRNA determination [3, 4], which shows fascinating advantages of rapid response, simplicity of operation and simple instrument. However, the signal outputs in the conventional DNA biosensors for microRNAs detection are generally based on single signal molecule labeling. This characteristic makes the analytical sensitivity not high enough to detect target microRNAs with an ultralow concentration in practical clinic diagnosis. To address this drawback, many nanomaterials such as Pd nanoparticles [5], gold nanoparticles [6], carbon nanomaterials [7] have been developed, which offers a new path to develop highly sensitive biosensors to satisfy the microRNAs analysis with higher demand.

Two-dimensional graphene oxide (GO) receives great interests as a fantastic carbon material in the fields of biomolecule sensing [8, 9], drug screening and delivery [10], energy storage [11] and bioimaging [12]. It has also been widely utilized as a smart biosensing material due to its stronger interaction with single-stranded DNA than the hybridized duplex or folded DNA. According to this feature, many GO-

Electronic supplementary material The online version of this article (https://doi.org/10.1007/s00604-018-3204-9) contains supplementary material, which is available to authorized users.

✉ Feng Gao
fgao1981@mnnu.edu.cn

[1] Department of Clinical Laboratory, Affiliated Hospital of Nantong University, Nantong, Jiangsu 226001, People's Republic of China

[2] College of Chemistry and Environment, Fujian Province Key Laboratory of Morden Analytical Science and Separation Technology, Minnan Normal University, Zhangzhou 363000, People's Republic of China

[3] Department of Gastroenterology and Clinical Laboratory, Nantong Third Hospital Affiliated to Nantong University, Nantong, Jiangsu 226006, People's Republic of China

Published online: 16 January 2019

based electrochemical and spectroscopic biosensors have been developed for analysis of various analytes such as bacteria [13] RNA [14], DNA [15], and heavy metal ions [16, 17]. Nevertheless, the GO cannot be directly utilized as electrochemical probe in electrochemical biosensors due to its electro-inactivity under the common condition. So, it is still a challenge to explore electroactive GO-based material to broaden its application. The introduction of electroactive signal molecules to GO is an appropriate strategy to obtain the materials bearing both good sensing capacity and excellent electrochemical signal.

Prussian Blue (PB, $Fe_4[Fe(CN)_6]_3{\cdot}xH_2O$), a typical mixed-valence metal (Fe^{II} and Fe^{III}) metal-organic framework has attracted considerable attention as signal molecule in electrochemical devices due to their excellent electro-activity [18]. Nevertheless, the low stability of PB at the neutral and weakly basic conditions limited its application [19]. The loading of PB on the other substrate such as carbon material is an effective strategy to improve the stability of PB in a wider acidic range [20]. The studies demonstrate that GO can be used as a useful substrate for direct growth of PB through successive adsorptions of Fe^{3+} and $Fe(CN)_6^{4-}$ [21, 22]. Through such a dipping method, the particle size, as well as uniformity of PB, can be well controlled, and the physicochemical properties such as mechanical strength and chemical stability of formed PB can be effectively improved.

Against above backgrounds, a novel electrochemical microRNA biosensor has been designed and constructed by applying probe DNA adsorbed GO as supporting matrix for direct growth of redox-active PB. When the sensor is interacted with target microRNA-122 to obtain rigid double helix structure, the GO with assembled PB will departure from the electrode surface due to weak affinity of GO with DNA/RNA hybrid. As a result, the electrochemical response of PB at the electrode surface will be reduced, and the target microRNA can also be effectively monitored. In addition, the biosensor has an outstanding capacity to distinguish target microRNA from other control microRNAs due to the smart recognition ability for hybridization reaction. The recovery assays reveal that the biosensor is reliable for microRNA-122 analysis in human serum samples, showing its promising application for clinic diagnosis of liver diseases.

Experimental

Reagents

Graphite, ethylenediamine tetraacetic acid (EDTA) and $K_4[Fe(CN)_6]{\cdot}3H_2O$ were purchased from Guangdong Xilong Chemical Co. Ltd. China (http://xilongchemical.en.made-in-china.com/). $FeCl_3{\cdot}6H_2O$ was provided by Shanghai Jiuyi Chemical Co., Ltd., China (http://jy-reagent.com/). 6-mercapto-1-hexanol (MCH) and Tris (2-carboxyethyl) phosphine hydrochloride (TCEP) was obtained from Sigma-Aldrich, China (https://www.sigmaaldrich.com/). The mixed phosphate obtained from Shanghai INESA Scientific Instrument Co. Ltd., China (http://en.inesa-instrument.com/), and used for preparing phosphate buffered saline (PBS, pH = 6.86). The GO was synthesized according to a modified Hummer's method [23], and the required dispersion of GO was prepared by dispersing an appropriate amount of GO in PBS under ultrasonication. Before use, the samples were diluted 20 times. All the solution in this work was prepared with doubly distilled water (DDW).

The 22-mer oligonucleotides probe, the target microRNA-122 and the other control microRNAs including microRNA-29 and microRNA-21 were provided by Sangon Bioengineering Co. Ltd. China (http://www.sangon.com/). The base sequences of all these oligonucleotides are listed as follows:

Probe DNA (pDNA): 5'-SH-CAA ACA CCA TTG TCA CAC TCC A-3';
MicroRNA-122: 5'-UGG AGU GUG ACA AUG GUG UUU G-3';
MicroRNA-29: 5'-UAG CAC CAU CUG AAA UCG GUU A-3';
MicroRNA-21: 5'-UAG CUU AUC AGA CUG AUG UUG A-3'.

The probe DNA solution was prepared by dissolving appropriate DNA with immobilization buffer (pH = 8.0) that consisted of 25 mM Tris-HCl, 10 mM TCEP, 100 mM NaCl, 100 mM $MgCl_2$. The other microRNA solutions were prepared with 10 mM Tris-EDTA buffer (pH = 8.0). All the oligonucleotide solutions were kept frozen when not in use.

Apparatus

The UV-Vis spectra were recorded on a Shimadzu UV-2550 spectrophotometer (Japan). Scanning electron microscopy (SEM) and atomic force microscopy (AFM) recorded on JEOL JSM-5600F Field-Emission (Japan) and Bruker Multimode 8 AFM (USA), respectively were used to characterize the surface morphology changes of the electrode upon fabrication of the biosensor. All the electrochemical tests including cyclic voltammetry (CV), electrochemical impedance spectroscopy (EIS) and differential pulse voltammetry (DPV) were performed on a Chenhua CHI 650C electrochemical analyzer (China) in connection with a conventional three-electrode system including a working electrode (gold electrode, Φ = 2 mm), a counter electrode (platinum wire) and a reference electrode (Ag/AgCl (3 M KCl)).

Fabrication of the sensing interface

Before fabrication, the gold electrode (AuE) was cleaned with the procedures of physical polishing with 0.05 μm α-Al_2O_3, chemical cleaning in Piranha solution prepared with concentrated sulfuric acid and 30% hydrogen peroxide in volume ratio of 7:3 for 20 min. Finally the electrode was electrochemical cleanned in 0.5 M H_2SO_4 with CV in the potential range between −0.2 V and 1.6 V (vs. Ag/AgCl (3 M KCl)) at a scan rate 0.05 V s^{-1}. After washed with DDW, the freshly cleaned AuE was dipped in 0.1 μM probe DNA solution for 24 h at 4 °C to obtain monolayer probe DNA modified AuE. After further rinsing with PBS and DDW for three times, the probe DNA modified electrode was immersed into 1 mM MCH at room temperature for 2 h to passivate the electrode surface that uncovered by probe DNA. The modified electrode was denoted as pDNA-MCH/AuE.

The assembly of GO was achieved by incubation of pDNA-MCH/AuE in 0.1 g L^{-1} GO solution for 3 h at 30 °C, and the electrode was signed as GO/pDNA-MCH/AuE. The direct growth of PB on GO/pDNA-MCH/AuE was performed by the following procedures: First, the mixture solution (solution 1) of 0.01 M $FeCl_3$, 0.1 M HCl and 0.1 M KCl and solution 2 containing 0.01 M $K_4[Fe(CN)_6]$, 0.1 M HCl and 0.1 M KCl were respectively prepared. Then the GO/pDNA-MCH/AuE was incubated in solution 1 for 1 min, DDW for 30 s, solution 2 for 60 s, and DDW for 30 s in turn. In this process, the temperature of all the solutions was kept at 30 °C to ensure the reproducibility of the sensor. After above process was repeated for seven cycles, the electrode was carefully rinsed with DDW and blow-dried with N_2 stream. Thus the electrochemical biosensor (PB/GO/pDNA-MCH/AuE) was achieved. In addition, to study the influence of GO for the direct growth of electroactive PB, the pDNA-MCH/AuE without pre-adsorption of GO was also used as the substrate for synthesis of PB by the same procedure, and the control electrode was denoted as PB/pDNA-MCH/AuE.

Hybridization reaction

The hybridization reaction of the biosensor with target microRNA was carried out by immersing the PB/GO/pDNA-MCH/AuE into 200 μL analyte solution with different concentrations of microRNA-122 for 60 min under 30 °C. Afterwards, the electrode was washed with PBS for 10 min to eliminate the physically attached microRNAs. To evaluate the specificity of the biosensor, the hybridizations of PB/GO/pDNA-MCH/AuE with 10 nM control microRNAs, i.e., microRNA-29 and microRNA-21 were carried out under the same condition and procedure.

Preparation of clinical serum samples and electrochemical measurements

The human serum samples were kindly provided by College of Biological Sciences and Technology of Minnan Normal University with ethical approval. The serum preparation was performed by standing the whole blood at room temperature for 4 h and then collecting pale yellow supernatant. The test solution of serum was obtained by injection 30 μL collected serum into 570 μL 10 mM Tris-EDTA buffer (pH = 8.0), yielding 20-fold diluted serum sample. Then 0.050 nM, 0.500 nM, 1.000 nM and 10.00 nM microRNA-122 standard solution were respectively spiked into above diluted serum solution. After sufficiently mixing, the biosensor was incubated in the serum solution for 60 min, and then rinsed with PBS. The electrochemical response of PB/GO/pDNA-MCH/AuE and its hybridization performance were monitored by CV and DPV in 0.1 M KCl. The reduction peak currents generated at 0.18 V (vs. Ag/AgCl (3 M KCl)) were adopted as the analytical signals.

Results and discussion

Choice of the materials

The biosensing strategy for microRNA-122 is realized by assembly of graphene oxide (GO) on probe electrode-confined DNA coupling with in-situ growth of Prussian blue (PB) (Scheme 1). GO is a versatile carbon nanomaterial. Compared with graphene, GO presents better hydrophilicity, biocompatibility and richer functional groups like -COOH and -OH. So, it is often served as a substrate for synthesis of biomaterials [24, 25]. On the other hand, it has been extensively reported that the GO has specific interaction with single-stranded DNA rather than hybridized DNA, due to the π-stacking interaction between GO and exposed bases on single-stranded DNA. Based on this feature, the GO has been utilized as an optical and electrochemical sensing material for DNA analysis [26, 27]. But the single component GO has an inferior electrochemical signal. So, the composite of GO with an electroactive molecule can be an ideal candidate for electrochemical sensing analysis of DNA or RNA. PB is an excellent electroactive material with intense redox signal and moderate redox potential. Also, the previous work reported that the GO can act as a substrate for in-situ growth of nanosized PB via a simple dipping method [21, 22]. This also inspires the idea to fabricate the GO/PB-based electrochemical sensing interface via the assembly of GO on probe DNA electrode, followed by in-situ growth of PB on GO. Thus, the composite of GO/PB simultaneously owns two functions, i.e., the good discrimination ability to probe DNA and hybridized DNA and excellent electrochemical output response.

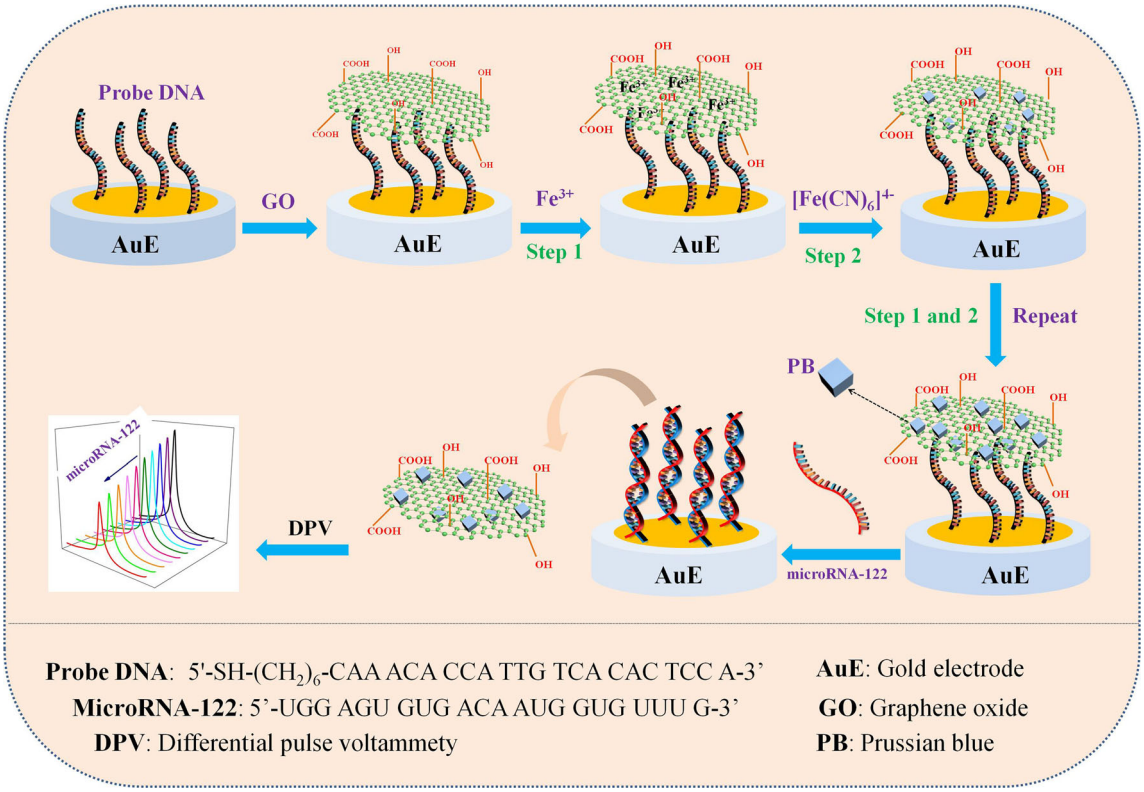

Scheme 1 The outlined strategy for electrochemical sensing detection of microRNA-122 based on direct growth of electroactive Prussian blue (PB) on GO attached on DNA probe electrode

Spectroscopic and morphology characterization

To probe direct synthesis of PB on GO, the electronic absorption spectrum of GO modified silica glass (GO/SG) upon successive dipping in solution 1 and solution 2 were measured. The UV-Vis spectra (Fig. S1) and the discussion are given in Electronic Supplementary Material. The assembly of GO on probe DNA modified electrode and the direct growth of PB on surface GO were also investigated by SEM (Fig. S2). The result evidently suggests that the GO can be effectively attached on probe DNA modified electrode and the adsorbed GO can be used as an effective substrate for the growth of PB with average size 100 nm.

In this work, the fabrication of the biosensing interface and its hybridization capacity with target microRNA are characterized by high-resolution scanning probe microscopy, atomic force microscope (AFM). Figure 1 shows the topographic (a), three-dimension (3D) (b), and cross-sectional (c) AFM results of the probe electrode before (A) and after successive assembly with GO (B), PB (C) and interaction with target microRNA-122 (D). It is found that the probe electrode is relatively smooth, and the largest height (H) and average roughness degree (R_a) are determined to be 21.75 nm and 7.29 nm, respectively. When GO is attached on the probe electrode, a large amount of hill-like peaks are observed, and the values of H and R_a are respectively increased to 51.67 nm and 14.7 nm. These results suggest that GO has been attached to pDNA modified electrode surface via interaction with pDNA. When the GO modified electrode is used as a supporting matrix for PB growth, it is observed that the electrode surface become rougher. The values of H and R_a are increased to 154.71 nm and 55.0 nm, respectively, confirming that the PB nanoparticles have been successfully prepared by the dipping method.

It is interesting that after hybridization of the sensing interface with microRNA-122, the values of H and R_a are respectively decreased to 65.37 nm and 26.6 nm. This result indicates that when the single-stranded probe DNA is hybridized with target microRNA to form double-stranded structure, the GO with the deposited PB fall off from the electrode due to the weak affinity between GO and DNA/RNA hybrid. So, the decrease of peak height and roughness of the biosensor upon interaction with target microRNA-122 testifies the hybridization feasibility of the PB/GO-based sensing interface for target microRNA.

Electrochemical behaviors of the biosensor

To better understand the inducing role of GO for the growth of PB, the redox response of the biosensor was studied and compared with that of the control electrode (PB/pDNA-MCH/AuE). Figure 2a shows the CVs of GO/pDNA-MCH/AuE in

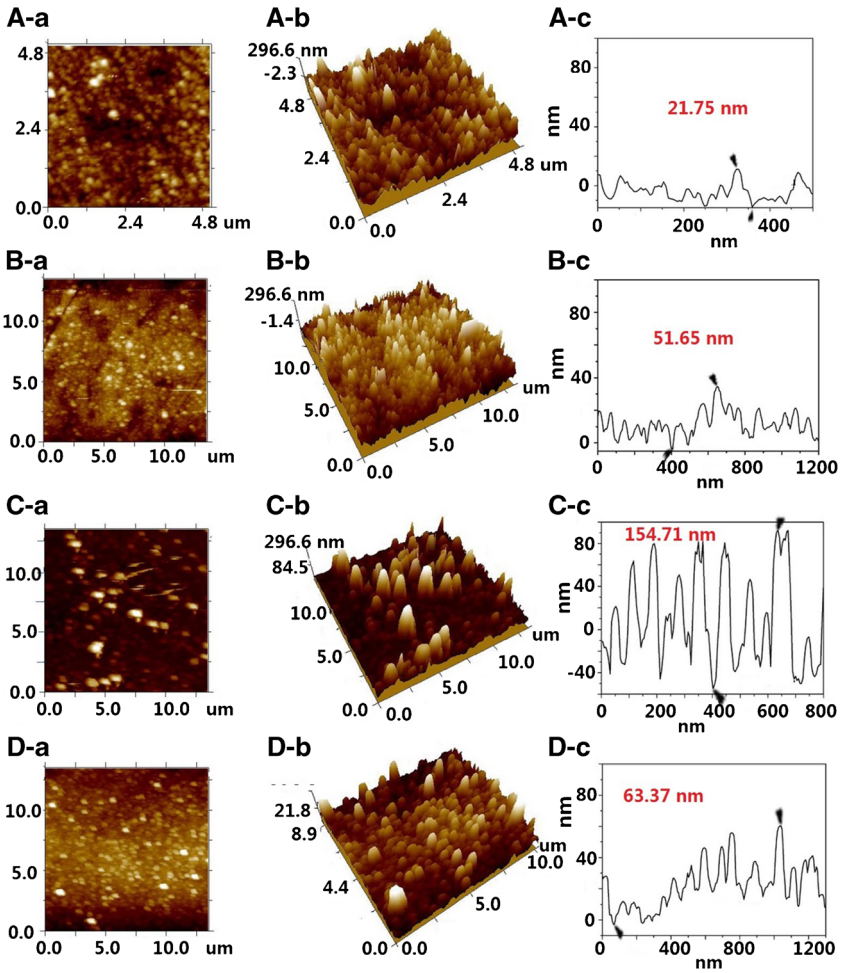

Fig. 1 Topographic (a), three-dimension (b), and cross-sectional (c) AFM images of the probe modified AuE before (A) and after successive assembly with GO (B), PB (C) and target microRNA-122 (D)

0.1 M KCl before and after deposition of PB. As showed in curve a, not any Farady signal is observed at GO/pDNA-MCH/AuE (curve a), showing that the supporting film of GO/pDNA-MCH at the electrode surface is silent in electrochemistry. However, after the alternative incubation of the electrode in solution 1 and solution 2 for 7 cycles, a couple of well-defined redox peaks that identical to the electrochemical response of PB [28, 29] is observed at +0.16 V and + 0.20 V (vs. Ag/AgCl (3 M KCl)) (curve b). This result demonstrates that PB has been successfully synthesized at the pDNA electrode surface and presents excellent redox response. However, only a couple of feeble redox peaks is observed at the control electrode of pDNA-MCH/AuE upon deposition with PB (curve c). Therefore, through comparison, it can be concluded that the GO material plays an important role to direct growth of electroactive PB as well as the enhancement of electrochemical signal due to its rich active sites and large surface area.

The influence of the scan rate (v) on redox behavior of PB directly grown at the electrode surface was further studied. As the results shown in Fig. 2b, with increase of v, the characteristic redox peaks of PB increase regularly. The redox peaks currents (I_p) presents good linear relationships with square root of scan rate ($v^{1/2}$) over the scan rate range from 10 mV s^{-1} to 350 mV s^{-1} (Inset of Fig. 2b), obeying the regression equations of I_{pc} (μA) = 45.0623$v^{1/2}$ (V/s) + 0.2185 (r = 0.9993) and I_{pa} (μA) = −29.6139$v^{1/2}$ (V/s) + 1.7394 (r = 0.9988). This phenomenon suggests that the electrochemical behaviors of PB grown on electrode-confined GO follows a diffusion-controlling process, rather than an adsorption-determined reaction. This can be explained by fact that the redox reaction of PB requires the presence of K^+ as described in the following equation [29]. The diffusion of K^+ from the bulk solution to the electrode surface is rate controlling step in the whole process.

$$\mathbf{Fe_4(III)\left[Fe(II)(CN)_6\right]_3 + 4e^- + 4K^+ \rightarrow K_4\,Fe_4(II)\left[Fe(II)(CN)_6\right]_3}$$

Optimization of experimental conditions

On the purpose of obtaining the optimal redox behavior and sensing performance, some conditions for the biosensor

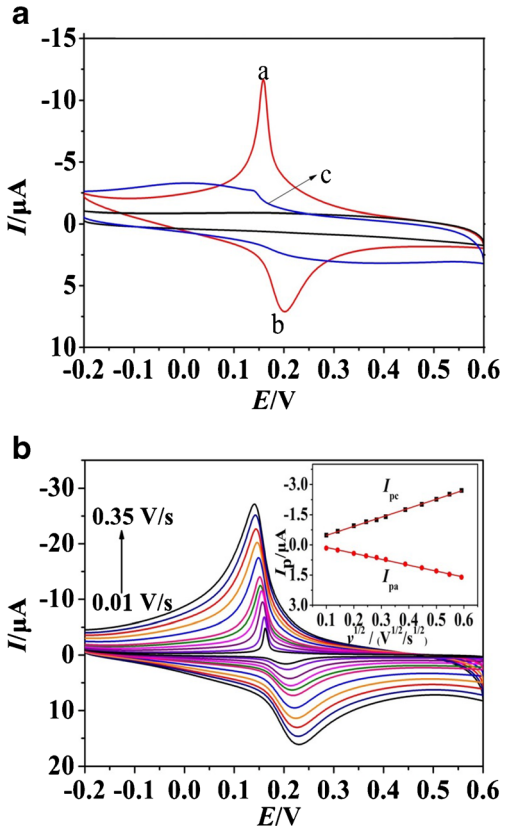

Fig. 2 **a** CVs of GO/pDNA-MCH/AuE (*a*), PB/GO/pDNA-MCH/AuE (*b*) and PB/pDNA-MCH/AuE (*c*) in 0.1 M KCl. Scan rate: 0.1 V s^{-1}. **b** CVs of PB in 0.1 M KCl solution at different scan rates (10, 20, 40, 60, 80, 100, 150, 200, 250, 300, 350 mV/s from inner to outer). Inset of is the plot of reduction and oxidation peak currents versus square root of the scan rate ($v^{1/2}$)

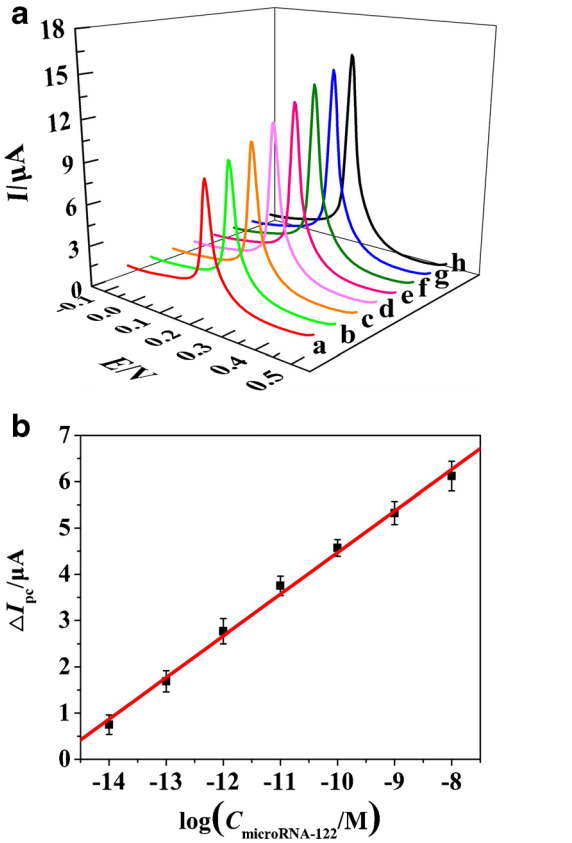

Fig. 3 **a** DPV response of the PB/GO/pDNA-MCH/AuE before (*a*) and after hybridization with 10 fM (*b*), 0.1 pM (*c*), 1.0 pM (*d*), 10 pM (*e*), 0.1 nM (*f*), 1.0 nM (*g*), 10 nM (*h*) microRNA-122 in 0.1 M KCl. **b** The relationship between -ΔI_{pc} and log$C_{microRNA-122}$. The standard deviation of three measurements was represented by the error bars. All the DPV data are collected in potentials ranging from 0.5 V to −0.1 V (vs. Ag/AgCl (3 M KCl)), and the values of I_{pc} are acquired at the potential of 0.18 V (vs. Ag/AgCl (3 M KCl))

preparation and hybridization reaction were optimized. The detailed results (Fig. S2) and discussion are presented in the Electronic Supplementary Material. Through optimization, the optimal conditions are summarized as follows: (1) Assembly time of GO on pDNA-MCH/AuE: 3 h; (2) Dipping cycles of GO/pDNA-MCH/AuE in solution 1 (0.01 M $FeCl_3$, 0.1 M HCl and 0.1 M KCl) and solution 2 (0.01 M $K_4[Fe(CN)_6]$, 0.1 M HCl and 0.1 M KCl): 7; (3) Hybridization of between the biosensor and microRNA-122: 60 min.

Analytical performance of the biosensor

Figure 3a shows DPV results of PB/GO/pDNA-MCH/AuE upon hybridization with different amounts of microRNA-122. It is clearly observed that the in-situ grown PB presents sharp reduction peaks at 0.18 V (vs. Ag/AgCl (3 M KCl)) during the analytical tests. The peak currents decrease gradually with the increase of the concentration of microRNA-122 ($C_{microRNA-122}$), which suggests that increasing amount of double-helix structured DNA-RNA has been achieved on the sensing surface. The difference values (ΔI_{pc}) of reduction peak currents of PB displays a good correlation with logarithmic values of $C_{microRNA-122}$ (lg$C_{microRNA-122}$) in the range from 10 fM to 10 nM, with the regression equation of -ΔI_{pc} (μA) =0.092(±0.0027)lg($C_{microRNA-122}$/M) + 1.4(±0.031) (r = 0.995, Fig. 3b). From the slope of the equation and the geometric surface area (0.0314 cm^2) of the electrode, the sensitivity of the analytical is determined to be 2.93 μA cm^{-2} dec^{-1}. Then the limit of detection (LOD) of the biosensor for microRNA-122 detection is estimated to be 1.5 fM. Table S1 lists the analytical performance of the sensor, and its comparison with the other microRNA biosensors. As seen, the GO/PB based sensor presents wider linear range and lower LOD, showing that the PB/GO/pDNA-MCH/AuE is more promising for the practical application in clinic analysis of microRNA. Such a low detection limit might be attributed to the following factors: (1) The high discriminating ability of GO toward DNA and DNA/RNA duplex structure causes outstanding signal output during hybridization reaction; (2) High electroactivity of PB and the nanosize effect of PB/GO composite make the biosensing interface having dual signal-

amplification function, therefore leading to higher sensitivity for target RNA detection.

Specificity, reproducibility, and stability

Figure 4a shows the DPVs and the corresponding bar chart (inset) for the reduction peaks of PB at GO/pDNA-MCH/AuE before and after hybridization with different microRNAs of microRNA-122, microRNA-29, microRNA-21, and the mixture of the three microRNAs. The largest signal change is obtained at microRNA-122 hybridized electrode due to the formation of intact DNA/RNA double-helix structure between pDNA and microRNA-122. In contrast, on the control microRNA-29 and microRNA-21 hybridized electrodes, the DPV signals are almost the same as that of the unhybridized electrode, suggesting that the sensor has no response to the two control microRNAs. In addition, when the biosensor was applied for the detection of the microRNA-122 in the presence of the other two control microRNAs, it is found that the response is very close to that of single-component of microRNA-122. All these results confirm that the PB/GO/pDNA-MCH/AuE owns excellent selectivity for distinguishing the target microRNA-122 from the other possibly coexisted microRNAs.

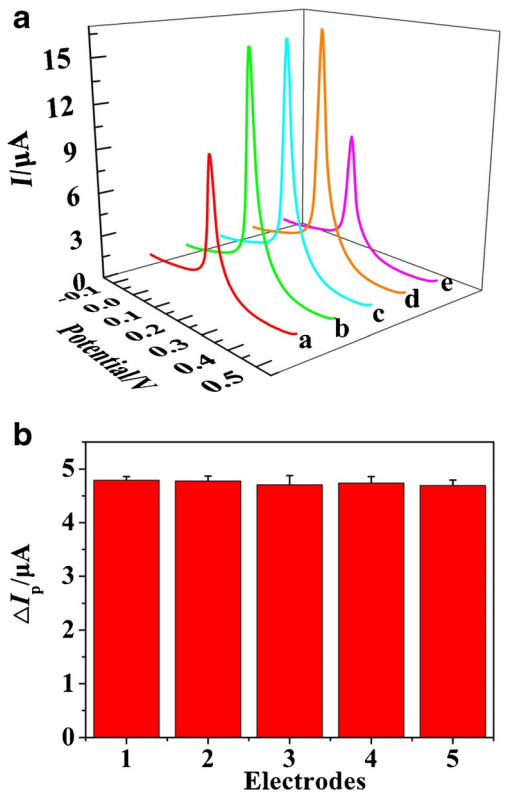

Fig. 4 **a** DPVs of probe electrode (*a*) upon hybridization with microRNA-29 (*b*), microRNA-21 (*c*), microRNA-122 (*d*), and the mixture of the three microRNAs (*e*). All the concentrations of hybridized sequences are 10 nM. **b** Reproducibility of the biosensor for the detection of microRNA-122. All the DPV data are collected in potentials ranging from −0.1 V to 0.5 V (vs. Ag/AgCl (3 M KCl)), and the values of I_{pc} are acquired at the potential of 0.18 V (vs. Ag/AgCl (3 M KCl)). The supporting electrolyte is 0.1 M KCl

The reproducibility and stability are also the critical performance of a biosensor in practical use. In this work, the reproducibility of the biosensor was investigated by detecting 1.0 nM target microRNA-122 with five parallel-made PB/GO/pDNA-MCH/AuE. The peak current variation (ΔI_{pc}) from DPV results are showed in Fig. 4b, from which it is observed that the values of ΔI_{pc} are close to each other and a relative standard deviation (RSD) of 2.5% ($n = 5$) is estimated. These results show that the DNA biosensor has an excellent reproducibility for target microRNA analysis. The stability of the biosensor was monitored by keeping the biosensor in the refrigerator (4 °C) with a cap covered on the top of the electrode and electrochemically measured every day. The result shows that only a decrease of 4.5% in peak current is obtained after 7 days, suggesting a good stability of the biosensor.

Analytical performance assessment in real biological samples

To assess reliability and accuracy of the biosensor in the practical clinical application, the biosensor was applied to detect microRNA-122 that spiked into 20-fold diluted healthy human serum samples. Figure 5 shows the DPV response of the biosensor in 0.1 M KCl after incubation in the sample without and with 10 nM microRNA-122. The results show that the DPV response obtained on the electrode after incubation in the blank sample (curve b) is almost identical to that of the pristine biosensor (curve a). This suggests the blank

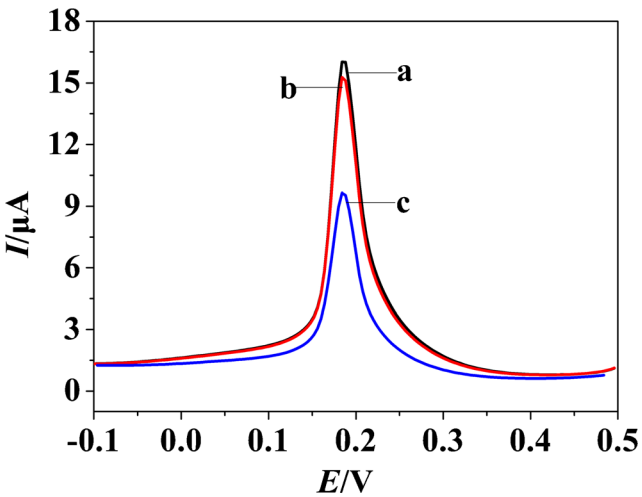

Fig. 5 DPVs of the biosensor before (*a*) and after incubation in 20-fold diluted blank serum (*b*) and 20-fold diluted serum containing 10 nM microRNA-122 (*c*). All the DPV data were collected in potentials ranging from 0.5 V to −0.1 V (vs. Ag/AgCl (3 M KCl)), and the supporting electrolyte is 0.1 M KCl

sample has no effect on the electrochemical response of the sensor. However, when the microRNA-122 is present in the solution, the reduction peak decrease obviously (curve c), indicating that the biosensor is feasible for recognition of target microRNA-122 in the complex serum sample. The accuracy of the biosensor was further assessed by recovery assay. The results show that when 0.05 nM, 0.5 nM, 1.0 nM and 10 nM microRNA-122 standard solution were respectively injected into 20-fold diluted serum samples, and measured three times for each sample, the recoveries and RSD are in the range of 97.2–103% and 2.2–3.2%, respectively (Table 1). These results confirm that the GO/PB-based biosensor has good precision and reliability for DNA analysis in real samples.

Conclusions

A novel electrochemical microRNA biosensor was developed on the basis of direct growth of electroactive PB on GO modified DNA electrode. The GO was attached on the probe DNA modified gold electrode via the π-stacking, and then the PB nanoparticles with excellent electroactivity were directly grown on the surface of GO via alternative dipping in Fe^{3+} and $Fe(CN)_6^{4-}$ solution. The smart use of GO in this work has two functions, i.e., acting a smart discriminator for the probe DNA and the hybridized DNA/RNA duplex; and a supporting platform for direct growth of PB nanoparticles. Due to the synergy of GO and PB in nanosizes, the biosensing interface presented intense electrochemical response as well as high sensitivity for target microRNA detection. The biosensor also presented excellent selectivity for target microRNA-122, suggesting that the PB-GO based sensing interface represents a promising clinical application for microRNA. Despite these advantages, the preparing time of the biosensor is still relatively long (24 h for probe DNA immobilization, 2 h for MCH assembly, and 3 h for GO adsorption), which cannot satisfy requirement for fast and real-time analysis. Therefore, further study should focus on the development of fast probe DNA immobilization method and GO assembly strategy.

Table 1 Determination of microRNA-122 spiked into human serum ($n = 3$) with the PB/GO-based biosensor

Sample	Spiked (nM)	Found (nM)	Recovery (%)	RSD (%)
1	0.050	0.0486	97.2%	3.2
2	0.500	0.494	98.8%	2.2
3	1.000	1.01	101%	3.1
4	10.00	10.03	103%	2.3

Acknowledgements This work was financially supported by the National Natural Science Foundation of China (Nos. 81873978, 81601842, 21802064), the Sixth Talent Peaks Project of Jiangsu Province (2018-WSW-068), the 64th grant of Chinese Post-doctoral Science Foundation (2018 M642298), and Foundation of Key Laboratory of Sensor Analysis of Tumor Marker from Ministry of Education, Qingdao University of Science and Technology.

Compliance with ethical standards The author(s) declare that they have no competing interests.

References

1. Kutay H, Bai S, Datta J, Motiwala T, Pogribny I, Frankel W, Jacob S-T, Ghoshal K (2006) Downregulation of miR-122 in the rodent and human hepatocellular carcinomas. J Cell Biochem 99:671–678. https://doi.org/10.1002/jcb.20982
2. Chen C-F, Ridzon D-A, Broomer A-J, Zhou Z-H, Lee D-H, Nguyen J-T, Barbisin M, Xu N-L, Mahuvakar V-R, Andersen M-R, Lao K-Q, Livak K-J, Guegler K-J (2005) Real-time quantification of microRNAs by stem-loop RT-PCR. Nucleic Acids Res 33: e179. https://doi.org/10.1093/nar/gni178
3. Smith D-A, Newbury L-J, Drago G, Bowen T, Redman J-E (2017) Electrochemical detection of urinary microRNAs via sulfonamide-bound antisense hybridisation. Sensors Actuators B Chem 253: 335–341. https://doi.org/10.1016/j.snb.2017.06.069
4. Chen A, Gui G-F, Zhuo Y, Chai Y-Q, Xiang Y, Yuan R (2015) Signal-off electrochemiluminescence biosensor based on Phi29 DNA polymerase mediated strand displacement amplification for microRNA detection. Anal Chem 87:6328–6334. https://doi.org/10.1021/acs.analchem.5b01168
5. Wu X-Y, Chai Y-Q, Yuan R, Su H-L, Han J (2013) A novel label-free electrochemical microRNA biosensor using Pd nanoparticles as enhancer and linker. Analyst 138:1060–1066
6. Tian L, Qian K, Qi J-X, Liu Q-Y, Yao C, Song W, Wang Y-H (2018) Gold nanoparticles superlattices assembly for electrochemical biosensor detection of microRNA-21. Biosens Bioelectron 99:564–570. https://doi.org/10.1016/j.bios.2017.08.035
7. Akbarnia A, Zare HR (2018) A voltammetric assay for microRNA-25 based on the use of amino-functionalized graphene quantum dots and ss- and ds-DNAs as gene probes. Microchim Acta 185: 503. https://doi.org/10.1007/s00604-018-3037-6
8. Elancheziyan M, Manoj D, Saravanakumar D, Thenmozhi K, Senthilkumar S (2017) Amperometric sensing of catechol using a glassy carbon electrode modified with ferrocene covalently immobilized on graphene oxide. Microchim Acta 184:2925–2932. https://doi.org/10.1007/s00604-017-2312-2
9. Gao F, Cai X, Wang X, Gao C, Liu S, Gao F, Wang Q (2013) Highly sensitive and selective detection of dopamine in the presence of ascorbic acid at graphene oxide modified electrode. Sensors Actuators B Chem 186:380–387. https://doi.org/10.1016/j.snb.2013.06.020
10. Oz Y, Barras A, Sanyal R, Boukherroub R, Szunerits S, Sanyal A (2017) Functionalization of reduced graphene oxide via thiol-maleimide "click" chemistry: facile fabrication of targeted drug delivery vehicles. ACS Appl Mater Interfaces 9:34194–34203. https://doi.org/10.1021/acsami.7b08433

11. Xu J-J, Wang K, Zu S-Z, Han B-H, Wei Z-X (2010) Hierarchical nanocomposites of polyaniline nanowire arrays on graphene oxide sheets with synergistic effect for energy storage. ACS Nano 4: 5019–5026. https://doi.org/10.1021/nn1006539
12. Zang Z-G, Zeng X-F, Wang M, Hu W, Liu C-R, Tang X-S (2017) Tunable photoluminescence of water-soluble AgInZnS-graphene oxide (GO) nanocomposites and their application in-vivo bioimaging. Sensors Actuators B Chem 252:1179–1186. https://doi.org/10.1016/j.snb.2017.07.144
13. Chinnappan R, AlAmer S, Eissa S, Rahamn A-A, Salah K-M-A, Zourob M (2018) Fluorometric graphene oxide-based detection of Salmonella enteritis using a truncated DNA aptamer. Microchim Acta 185:61. https://doi.org/10.1007/s00604-017-2601-9
14. Li F, Chao J, Li ZH, Xing S, Su S, Li X-X, Song S-P, Zuo X-L, Fan C-H, Liu B, Huang W, Wang L-H, Wang L-H (2015) Graphene oxide-assisted nucleic acids assays using conjugated polyelectrolytes-based fluorescent signal transduction. Anal Chem 87:3877–3883. https://doi.org/10.1021/ac504658a
15. Dong H-F, Zhang J, Ju H-X, Lu H-T, Wang S-Y, Jin S, Hao K-H, Du H-W, Zhang X-J (2012) Highly sensitive multiple microRNA detection based on fluorescence quenching of graphene oxide and isothermal strand-displacement polymerase reaction. Anal Chem 84:4587–4593. https://doi.org/10.1021/ac300721u
16. Wen Y-Q, Xing F-F, He S-J, Song S-P, Wang L-H, Long Y-T, Li D, Fan C-H (2010) A graphene-based fluorescent nanoprobe for silver (I) ions detection by using graphene oxide and a silver-specific oligonucleotide. Chem Commun 46:2596–2598. https://doi.org/10.1039/B924832C
17. Zhang H, Jia S-S, Lv M, Shi J-Y, Zuo X-L, Su S, Wang L-H, Huang W, Fan C-H, Huang Q (2014) Size-dependent programming of the dynamic range of graphene oxide-DNA interaction-based ion sensors. Anal Chem 86:4047–4051. https://doi.org/10.1021/ac500627r
18. Pandey P-C, Panday D (2016) Tetrahydrofuran and hydrogen peroxide mediated conversion of potassium hexacyanoferrate into prussian blue nanoparticles: application to hydrogen peroxide sensing. Electrochim Acta 190:758–765. https://doi.org/10.1016/j.electacta.2015.12.188
19. Curulli A, Valentini F, Orlanduci S, Terranova M-L, Palleschi G (2004) Pt based enzyme electrode probes assembled with prussian blue and conducting polymer nanostructures. Biosens Bioelectron 20:1223–1232. https://doi.org/10.1016/j.bios.2004.06.026
20. Cinti S, Arduini F, Vellucci G, Cacciotti L, Nanni F, Moscone D (2014) Carbon black assisted tailoring of prussian blue nanoparticles to tune sensitivity and detection limit towards H_2O_2 by using screen-printed electrode. Electrochem Commun 47:63–66. https://doi.org/10.1016/j.elecom.2014.07.018
21. Qiu W-W, Zhu Q-H, Gao F, Gao F, Huang J-F, Pan Y-T, Wang Q-X (2017) Graphene oxide directed in-situ synthesis of Prussian blue for non-enzymatic sensing of hydrogen peroxide released from macrophages. Mater Sci Eng C 72:692–700. https://doi.org/10.1016/j.msec.2016.11.134
22. Liu X-W, Yao Z-J, Wang Y-F, Wei X-W (2010) Graphene oxide sheet-prussian blue nanocomposites: green synthesis and their extraordinary electrochemical properties. Colloids Surf B 81:508–512. https://doi.org/10.1016/j.colsurfb.2010.07.049
23. Hummers W-S, Offeman R-E (1958) Preparation of graphitic oxide. J Am Chem Soc 80:1339–1339. https://doi.org/10.1021/ja01539a017
24. Wang Y, Chen J-T, Yan X-P (2013) Fabrication of transferrin functionalized goldnanoclusters/graphene oxide nanocomposite forturn-on near-infrared fluorescent bioimaging of cancercells and small animals. Anal Chem 85:2529–2535. https://doi.org/10.1021/ac303747t
25. Zhao R-T, Lv M, Li Y, Sun M-X, Kong W, Wang L-H, Song S-P, Fan C-H, Jia L-L, Qiu S-F, Sun Y-S, Song H-B, Hao R-Z (2017) Stable nanocomposite based on pegylated and silver nanoparticles loaded graphene oxide for long-term antibacterial activity. ACS Appl Mater Interfaces 9:15328–15341. https://doi.org/10.1021/acsami.7b03987
26. Bonanni A, Chua C-K, Zhao G-J, Sofer Z, Pumera M (2012) Inherently electroactive graphene oxide nanoplatelets as labels for single nucleotide polymorphism detection. ACS Nano 6:8546–8551. https://doi.org/10.1021/nn301359y
27. Liu CJ-Y, Seo T-S (2010) Graphene oxide arrays for detectingspecific DNA hybridization by fluorescence resonance energy transfer. Biosens Bioelectron 25:2361–2365. https://doi.org/10.1016/j.bios.2010.02.022
28. Zhao J-H, Yue P-W, Tricard S, Pang T, Yang Y, Fang J (2017) Prussian blue (PB)/carbon nanopolyhedra/polypyrrole composite as electrode: a high performance sensor to detect hydrazine with long linear range. Sensors Actuators B Chem 251:706–712. https://doi.org/10.1016/j.snb.2017.05.042
29. Kuhnhardt C (1994) Nucleation and growth of prussian blue films on glassy carbon electrodes. J Electroanal Chem 369:71–78. https://doi.org/10.1016/0022-0728(94)87083-7